Pentacene-Based Polycyclic Aromatic Hydrocarbon Dyads with Cofacial Solid-State Ï-Stacking

ARTICLE *in* CHEMISTRY - A EUROPEAN JOURNAL · OCTOBER 2009

Impact Factor: 5.73 · DOI: 10.1002/chem.200902179 · Source: PubMed

5 AUTHORS, INCLUDING:

Dan Lehnherr
Cornell University
17 PUBLICATIONS **274** CITATIONS

SEE PROFILE

CHEMISTRY
A EUROPEAN JOURNAL

DOI: 10.1002/chem.200902179

Pentacene-Based Polycyclic Aromatic Hydrocarbon Dyads with Cofacial Solid-State π-Stacking

Dan Lehnherr,[a] Adrian H. Murray,[a] Robert McDonald,[b] Michael J. Ferguson,[b] and Rik R. Tykwinski*[a, c]

Polycyclic aromatic hydrocarbons (PAHs) are a class of compounds that has received attention from the fields of organic chemistry, materials chemistry, theoretical chemistry, cancer research, environmental science, and astronomy.[1] In particular, PAHs play a significant role as materials for organic electronics applications, and their properties have been tuned for applications such as light-emitting diodes, field effect transistors, photovoltaic cells, and sensors.[2] Short linearly-fused acenes such as naphthalene, anthracene, and tetracene (naphthacene) are reasonably stable and their semiconducting properties have been systematically studied. On the other hand, larger acenes such as hexa-, and heptacene necessitate functionalization to obtain stable materials[3] and little has been reported concerning their semiconductive performance. When appropriately functionalized, pentacene seems to strike a balance between these two extremes: it shows intriguing charge-transport abilities, while still offering the prospect for stable, processable materials. For this and other reasons, pentacene derivatives continue to be a rich source of discovery in the field of organic semiconductors.[2]

Ideally, organic materials for solar cell applications would absorb light throughout the solar spectrum.[4] This requires materials with electronic absorption spectra covering a wide range of energies across the UV/Vis spectrum and into the near-IR. Unfortunately, functionalized pentacenes such as 6,13-bis(triisopropylsilylethynyl)pentacene (**1**) typically have a very narrow absorption region in the ultraviolet (centered around ca. 310 nm) in addition to absorption bands in the visible region of 525–660 nm; they are quite transparent in the region of 350–525 nm.[5] Thus, a homologous series of pentacene–PAH dyads (**2a–f**, Scheme 1) has been realized in which the absorption is tuned in the visible region of the spectrum.[6] The design of these targets is based on three key factors. First, a PAH should be attached to the pentacene through an ethynyl linker at the 13-position to provide extended conjugation and enhance absorption in the 300–475 nm range.[7] Second, the increased π-surface provided by the PAH moiety should offer improved π-stacking interactions in the solid-state. Finally, a triisopropylsilylethynyl group should be appended to the 6-position to maintain the solubility of the product. The results of this study are communicated herein, including the synthesis of dyads **2a–f** and a description of their absorption, emission, and electrochemical properties. Furthermore, motivated by the model for the solid-state packing developed by Anthony and co-workers for 6,13-bisfunctionalized pentacenes,[5] the X-ray crystallographic data of dyads **2b–d** and **2f** have been analyzed.[8]

The two-step synthesis of pentacene-based dyads **2a–f** is shown in Scheme 1. Deprotonation of the corresponding terminal acetylene with HexLi gave acetylides **3a–e**, which were then added to a solution of **4**[8e,9] in THF to afford diols **5a–e** in good yields (83–99%). For the synthesis of diol **5f**, anthraceneacetylide **3f** was formed by the reaction of 9-(trimethylsilylethynyl)anthracene with MeLi to avoid isolation of 9-ethynylanthracene. Finally, the Sn^{II}-mediated reduction of **5a–f** afforded conjugated pentacene dyads **2a–f** in good yields of 83–98%.

Dyads **2a–d** are sufficiently soluble for purification by column chromatography, while the less soluble pyrenyl **2e** and anthryl **2f** derivatives were purified by precipitation. The stability of these materials was assessed by thermal gravimetric analysis (TGA) and differential scanning calorimetry (DSC, Table 1). Although TGA does not show any

[a] D. Lehnherr, A. H. Murray, Prof. Dr. R. R. Tykwinski
Department of Chemistry, University of Alberta
Edmonton, Alberta, T6G 2G2 (Canada)

[b] Dr. R. McDonald, Dr. M. J. Ferguson
X-Ray Crystallography Laboratory
Department of Chemistry, University of Alberta
Edmonton, Alberta, T6G 2G2 (Canada)

[c] Prof. Dr. R. R. Tykwinski
New address: Institut für Organische Chemie
Friedrich-Alexander-Universität
Erlangen-Nürnberg, Henkestrasse 42, 91054 Erlangen (Germany)
E-mail: rik.tykwinski@chemie.uni-erlangen.de

Supporting information for this article is available on the WWW under http://dx.doi.org/10.1002/chem.200902179.

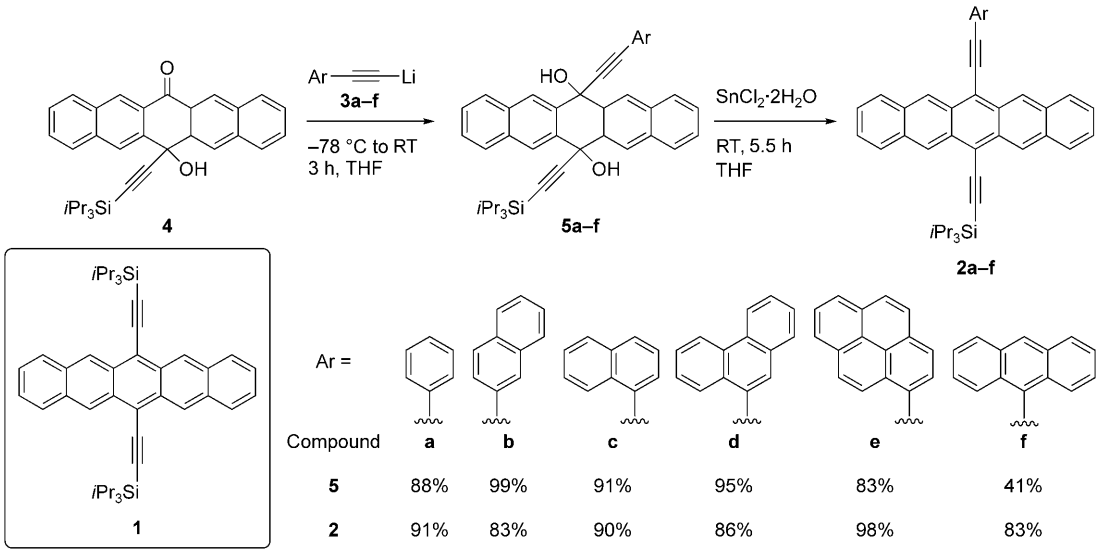

Scheme 1. Synthesis of pentacene-based PAH dyads **2a–f**.

Table 1. Thermal analysis of dyads **2a–f**.

Compound	TGA	DSC (decomposition)	
	T_d [°C]	onset [°C]	peak [°C]
2a	435	174	180
2b	435	190	197
2c	420	206	210
2d	425	218	221
2e	420	248	256
2f	390	270	271

significant weight loss (<5%) below 390°C for **2a–f**, DSC reveals decomposition occurs at much lower temperatures.[10] In general, thermal stability increases as the PAH substituent appended to the pentacene becomes larger. Furthermore, the geometry of the PAH affects the stability as well: a parallel arrangement of the acene (i.e., 1-naphthyl **2c** and anthryl **2f**) provides improved stability in comparison to a non-parallel geometry (i.e., 2-naphthyl **2b** and phenanthryl **2d**).[11]

UV/Vis spectroscopy (in CH_2Cl_2) was used to explore the electronic outcome of varying the PAH partner connected to the pentacene moiety (Figure 1, Table 2). In principle, the ethynyl linker in **2a–f** should facilitate electronic communication between the PAH pairs. Consistent with this expectation, a red shift is observed in λ_{max} values for **2a–f** as the pendent PAH chromophore is formally increased in size. The effect is, however, relatively small upon moving from **2a** (λ_{max}=652 nm) to **2f** (λ_{max}=671 nm). More interesting effects are observed in the mid-energy absorption range between 325–500 nm, as absorptions (Table 2, λ_{mid}) are substantially red-shifted with increasing size of the pendent PAH group (Figure 1b). Thus, the structural evolution in the acene series from phenyl **2a** (λ_{mid}=360 nm) to naphthyl **2c** (λ_{mid}=395 nm) to anthryl **2f** (λ_{mid}=465 nm) demonstrates a red shift of over 100 nm for this absorption.

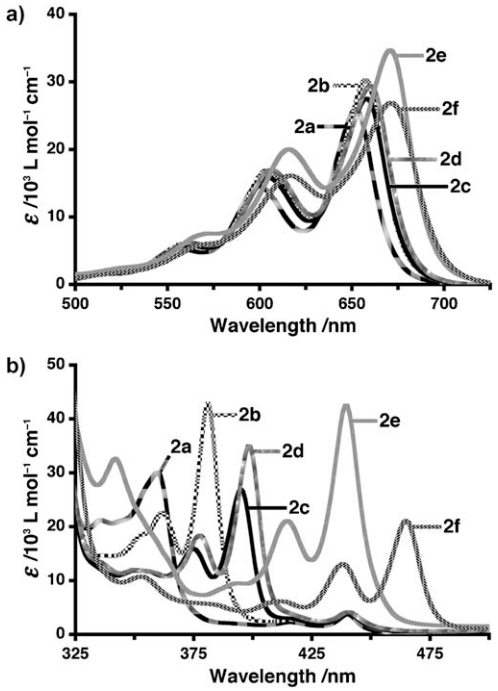

Figure 1. Solution-state UV/Vis absorption spectra for dyads **2a–f** in CH_2Cl_2. a) Low-energy region (500–725 nm) and b) mid-energy region (325–500 nm) of spectra.

Solid-state UV/Vis absorption spectra for thin films of pentacenes **2a–f** feature red shifts of 19 to 41 nm for the longest wavelength absorption λ_{max} in comparison to solution-state data in CH_2Cl_2 (Table 2).[12] Pentacenes bearing larger PAH moieties, such as pyrenyl **2e** and anthryl **2f**, show the largest red shifts, indicating more significant electronic coupling between molecules in the solid state. This observation is qualitatively in agreement with the X-ray crystallographic data currently available (vide infra).

Table 2. UV/Vis absorption and emission properties for dyads **2a–f**.

Compound	λ_{mid}[a] (in CH_2Cl_2) [nm]	λ_{max}[b] (in CH_2Cl_2) [nm]	λ_{max} (thin film) [nm]	$\lambda_{max,\,em}$ (in CH_2Cl_2) [nm]	Stokes shift [nm][c]	Φ_F[d] (in CH_2Cl_2)
2a	360	652	671	661	9	0.13
2b	381	657	679	667	10	0.12
2c	395	658	679	668	10	0.12
2d	398	660	686	670	10	0.11
2e	440	671	712	681	10	0.07
2f	465	671	712	688	17	0.006

[a] Wavelength of most intense absorption in the range of 325–500 nm. [b] Lowest energy absorption maxima. [c] Based on solution-state measurements. [d] Measured by using $\lambda_{exc}=551$ nm (see ref. [13]).

Solution-state emission in CH_2Cl_2 of pentacenes **2a–f** has been explored with an excitation wavelength (λ_{exc}) of 551 nm (Table 2).[12,13] Dyads **2a–e** have an emission quantum yield (Φ_F), of about 0.12 and a Stokes shift of ca. 10 nm. The anthryl derivative **2f**, however, shows both a significantly lower $\Phi_F=0.006$ and a larger Stokes shift of 17 nm, and this behavior is analogous to the essentially non-fluorescent conjugated pentacenes dimers recently reported.[6e] Finally, the emission energy and peak shape for all derivatives are largely unaffected by the choice of excitation wavelength (i.e., $\lambda_{exc}=551$ nm, the strongest mid-energy band, or strongest high energy band at ca. 310 nm).[12]

Cyclic voltammetry provides insight into how the PAH partner appended to the pentacene framework influences the HOMO and LUMO energies. It also allows for a comparison of band gaps obtained from solution-state UV/Vis data via the absorption edge (Table 3).[14] Pentacene derivatives **2a–d** show two reduction and one oxidation potentials, all three of which are reversible. In addition to two reversible reduction waves, pentacenes **2e** and **2f** also show two oxidation waves, although only the first is reversible. While both the reduction and the oxidation potentials decrease slightly as the size of the pendent PAH increased, there is surprisingly little variation in either the first oxidation or reduction potentials. The second reduction potential shows a marginal dependence on structure, deceasing from −1.90 V for **2a** to −1.77 V for **2f**. Overall, the trend for the electrochemical HOMO–LUMO gap determined by the CV data ($E_g^{electro}$) is reasonably consistent with that determined from the UV/Vis data (E_g^{opt}). This suggests that the energy of the HOMO is raised while the LUMO energy is lowered as benzannulation is increased along the series.

Table 3. Summary of redox and band gap data for dyads **2a–f**.[a]

Compound	E_{red1} [V]	E_{red2} [V]	E_{ox1} [V]	$E_g^{electro}$ [eV]	E_g^{opt}[b] [eV]
2a	−1.44	−1.90	0.39	1.83	1.81
2b	−1.42	−1.86	0.38	1.80	1.79
2c	−1.42	−1.86	0.39	1.81	1.79
2d	−1.40	−1.83	0.38	1.79	1.78
2e	−1.40	−1.80	0.34	1.74	1.74
2f[c]	−1.38	−1.77	0.33	1.71	1.74

[a] Cyclic voltammetry was performed in benzene/MeCN (3:1 v/v) solutions containing 0.1 M nBu$_4$NPF$_6$ as electrolyte at a scan rate of 150 mV s^{-1}. Potentials are referenced to the ferrocenium/ferrocene (Fc^+/Fc) couple used as an internal standard. [b] See ref. [14]. [c] Measured at a scan rate of 200 mV s^{-1}.

Solid-state packing of the PAH dyads has been investigated by using X-ray crystallography. Suitable single crystals of the 1-naphthyl (**2c**),[15] phenanthryl (**2d**),[16] and anthryl (**2f**)[17] derivatives are obtained relatively easily by slow evaporation from solutions in CH_2Cl_2 layered with acetone. On the other hand, crystals of the 2-naphthyl derivative **2b**[18] are obtained by slow evaporation of a solution in $CDCl_3$. Under analogous conditions, the phenyl derivative **2a** and the pyrenyl derivative **2e** afford fibrous bundles unsuitable for X-ray crystallographic analysis. The derivatives **2b–d** and **2f** crystallize with the PAH moiety coplanar or nearly coplanar with the pentacene moiety giving centrosymmetric or pseudo-centrosymmetric face-to-face dimers. In three cases (**2b**, **2d**, **2f**), long-range face-to-face π-stacking interactions are also observed.

Unlike for **2b**, **2d**, and **2f**, the crystallographic analysis of 1-naphthyl derivative **2c** (Figure 2a) shows no long-range π-stacking. The unit cell of **2c** contains two crystallographically independent molecules, and the naphthyl and pentacenyl moieties are nearly coplanar in both cases, with torsion angles between the acene moieties of 10–11°.[19] The solid-state packing of **2c** shows cofacial π-stacking interactions between the naphthyl and pentacenyl moieties of neighboring molecules with intermolecular C···C distances as small as 3.4 Å. There is, however, no long-range cofacial π-stacking; rather a herringbone arrangement is observed that features intermolecular edge-to-face interactions with a C–H···C(π) distance of 2.9 Å (H16A and C4B′, see Figure 2a). This is comparable with the edge-to-face interaction in one of the solid-state morphologies of pristine pentacene with a C–H···C(π) distance of 2.92 Å.[20]

The structure of 2-naphthylpentacene **2b** also contains two crystallographically independent molecules in the unit cell (Figure 2b). In molecule A, the naphthyl and pentacenyl moieties are coplanar (torsion angle of 0.8°), whereas for molecule B this angle is 8.2°.[19] The two crystallographically independent molecules of **2b** form a pseudo-centrosymmetric dimeric pair, and neighboring pairs are then stacked in a 1D columnar arrangement that provides long-range order. The intermolecular separation between neighboring molecules A and B, both within a dimeric pair and between dimeric pairs, is estimated to be 3.4 Å.[21]

Phenanthryl derivative **2d** crystallizes with a negligible torsion angle of 1.5° between the two PAH moieties in each dyad (Figure 2c).[19] Adjacent molecules form centrosymmetric dimeric pairs (e.g., bottom two molecules in Figure 2c) separated by an interplanar distance of 3.25 Å. Adjacent dimers then pack in a 1D slipped-stack arrangement with an interplanar distance of 3.32 Å (top two molecules in Figure 2c).[22]

Finally, the solid-state packing of anthryl derivative **2f** (Figure 2d) mirrors that of **2d**. The PAH moieties are essentially coplanar within each molecule (torsion angle of 1.2°),[19] and neighboring molecules form a centrosymmetric

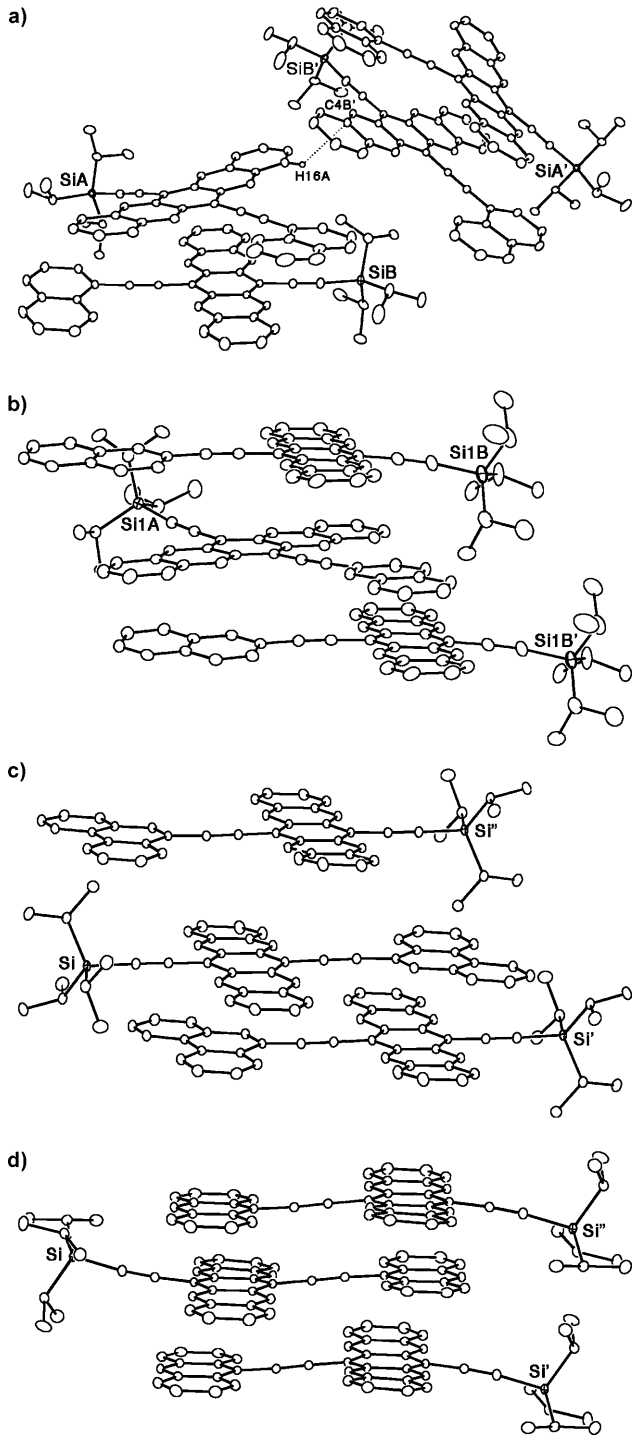

Figure 2. ORTEP representation illustrating the packing interactions in pentacene derivative a) **2c**, b) **2b**, c) **2d**, d) **2f**. Hydrogen atoms have been omitted from the structures for clarity. For cases where there are two crystallographically independent molecules (i.e., **2c** and **2b**), the Si atoms have been labeled with the letters A and B to denote molecules A and B.

pair with an interplanar distance of 3.26 Å (e.g., bottom two molecules in Figure 2d). These centrosymmetric dimers pack in 1D columnar stacks with an interplanar distance of 3.51 Å between each pair (top two molecules in Figure 2d).[22]

In summary, we demonstrate an efficient, stepwise route to unsymmetrically 6,13-disubstituted pentacenes for the formation of pentacene-based PAH dyads. The formal benzannulation of phenylpentacene **2a** provides pentacenes **2b–f**, which exhibit intermolecular cofacial π-stacking between the pentacene and the PAH moiety. The choice of the PAH moiety, as well as the point of attachment to the 6,13-diethynylated pentacene group, offers the ability to manipulate solid-state packing as well as the electronic properties as documented by both cyclic voltammetry and UV/Vis absorption/emission experiments. X-ray crystallography nicely shows that with increasing size of the pendent PAH group in **2b–d** and **2f**, cofacial packing is maximized between nearest neighbors. This fact should ultimately provide for a larger transfer integral, and, thus, enhanced conduction and improved charge-carrier mobility.[23]

Acknowledgements

This work has been generously supported by the University of Alberta, the Natural Sciences and Engineering Research Council of Canada (NSERC) through the Discovery grant program, and the Canadian Foundation for Innovation (CFI). We thank Dr. Khalid Azyat for kindly donating the pyrene starting material. D.L. thanks NSERC (PGS-D), the Alberta Ingenuity Fund (AIF), the Alberta Heritage Fund, the Killam Trusts, and the University of Alberta for scholarship support. A.H.M. thanks NSERC (PGS-D), AIF, and the University of Alberta for scholarship support.

Keywords: conjugation · hydrocarbons · oligomerization · pi interactions · semiconductors

[1] R. G. Harvey in *Polycyclic Aromatic Hydrocarbons*, Wiley-VCH, Weinheim, **1997**.

[2] a) M. Bendikov, F. Wudl, D. F. Perepichka, *Chem. Rev.* **2004**, *104*, 4891–4945; b) J. E. Anthony, *Chem. Rev.* **2006**, *106*, 5028–5048; c) J. E. Anthony, *Angew. Chem.* **2008**, *120*, 460–492; *Angew. Chem. Int. Ed.* **2008**, *47*, 452–483; d) A. R. Murphy, J. M. J. Fréchet, *Chem. Rev.* **2007**, *107*, 1066–1096.

[3] a) M. M. Payne, S. R. Parkin, J. E. Anthony, *J. Am. Chem. Soc.* **2005**, *127*, 8028–8029; b) R. Mondal, B. K. Shah, D. C. Neckers, *J. Am. Chem. Soc.* **2006**, *128*, 9612–9613; c) R. Mondal, R. M. Adhikari, B. K. Shah, D. C. Neckers, *Org. Lett.* **2007**, *9*, 2505–2508; d) D. Chun, Y. Cheng, F. Wudl, *Angew. Chem.* **2008**, *120*, 8508–8513; *Angew. Chem. Int. Ed.* **2008**, *47*, 8380–8385; e) I. Kaur, N. N. Stein, R. P. Kopreski, G. P. Miller, *J. Am. Chem. Soc.* **2009**, *131*, 3424–3425.

[4] a) S.-C. Lo, P. L. Burns, *Chem. Rev.* **2007**, *107*, 1097–1116; b) M. C. Scharber, D. Mühlbacher, M. Koppe, P. Denk, C. Waldauf, A. J. Heeger, C. J. Brabec, *Adv. Mater.* **2006**, *18*, 789–794; c) C. J. Brabec, N. S. Sariciftci, J. C. Hummelen, *Adv. Funct. Mater.* **2001**, *11*, 15–26.

[5] a) J. E. Anthony, J. S. Brooks, D. L. Eaton, S. R. Parkin, *J. Am. Chem. Soc.* **2001**, *123*, 9482–9483; b) J. E. Anthony, D. L. Eaton, S. R. Parkin, *Org. Lett.* **2002**, *4*, 15–18.

[6] For pentacene oligo- and polymers, see: a) S. Tokito, K.-H. Weinfurtner, H. Fujikawa, T. Tsutsui, Y. Taga, *Proc. SPIE-Int. Soc. Opt. Eng.* **2001**, *4105*, 69–74; b) T. Okamoto, Z. Bao, *J. Am. Chem. Soc.* **2007**, *129*, 10308–10309; c) D. Lehnherr, R. R. Tykwinski, *Org. Lett.* **2007**, *9*, 4583–4586; d) T. Okamoto, Y. Jiang, F. Qu, A. C. Mayer,

J. E. Parmer, M. D. McGehee, Z. Bao, *Macromolecules* **2008**, *41*, 6977–6980; e) D. Lehnherr, J. Gao, F. A. Hegmann, R. R. Tykwinski, *Org. Lett.* **2008**, *10*, 4779–4782; f) D. Lehnherr, R. McDonald, M. J. Ferguson, R. R. Tykwinski, *Tetrahedron* **2008**, *64*, 11449–11461; g) D. Lehnherr, J. Gao, F. A. Hegmann, R. R. Tykwinski, *J. Org. Chem.* **2009**, *74*, 5017–5024.

[7] a) B. Milián Medina, J. E. Anthony, J. Gierschner, *ChemPhysChem* **2008**, *9*, 1519–1523; b) I. Kaur, W. Jia, R. P. Kopreski, S. Selvarasah, M. R. Dokmeci, C. Pramanik, N. E. McGruer, G. P. Miller, *J. Am. Chem. Soc.* **2008**, *130*, 16274–16286.

[8] For X-ray crystallographic structures of unsymmetrical pentacenes, see: a) T. Takahashi, M. Kitamura, B. Shen, K. Nakajima, *J. Am. Chem. Soc.* **2000**, *122*, 12876–12877; b) C. R. Swartz, S. R. Parkin, J. E. Bullock, J. E. Anthony, A. C. Mayer, G. G. Malliaras, *Org. Lett.* **2005**, *7*, 3163–3166; c) T. Takahashi, S. Li, W. Huang, F. Kong, K. Nakajima, B. Shen, T. Ohe, K-i. Kanno, *J. Org. Chem.* **2006**, *71*, 7967–7977; d) Y.-M. Wang, N.-Y. Fu, S.-H. Chan, H.-K. Lee, H. N. C. Wong, *Tetrahedron* **2007**, *63*, 8586–8597; e) D. Lehnherr, R. McDonald, R. R. Tykwinski, *Org. Lett.* **2008**, *10*, 4163–4166; f) Y.-F. Lim, Y. Shu, S. R. Parkin, J. E. Anthony, G. G. Malliaras, *J. Mater. Chem.* **2009**, *19*, 3049–3056.

[9] A. Boudebous, E. C. Constable, C. E. Housecroft, M. Neuburger, S. Shaffner, *Acta Crystallogr. Sect. C* **2006**, *62*, o243-o245.

[10] Under an inert atmosphere, thermal decomposition of 6,13-diethynylated pentacenes has been attributed to the Diels–Alder reaction between the alkyne and the pentacene chromophore, while photochemical decomposition leads to [4+4] intermolecular dimerization similar to anthracene. See: a) M. M. Payne, S. A. Odom, S. R. Parkin, J. E. Anthony, *Org. Lett.* **2004**, *6*, 3325–3328; b) P. Coppo, S. G. Yeates, *Adv. Mater.* **2005**, *17*, 3001–3005; c) Y. Kim, J. E. Whitten, T. M. Swager, *J. Am. Chem. Soc.* **2005**, *127*, 12122–12130; d) S. H. Chan, H. K. Lee, Y. M. Wang, N. Y. Fan, X. M. Chen, Z. W. Cai, H. N. C. Wong, *Chem. Commun.* **2005**, 66–68; e) J. Chen, S. Subramanian, S. R. Parkin, M. Siegler, K. Gallup, C. Haughn, D. C. Martin, J. E. Anthony, *J. Mater. Chem.* **2008**, *18*, 1961–1969.

[11] For a study of substituent-size effects on solid-state packing and electronic influence on stability, see: a) reference [5b,7b,10e]; b) B. H. Northrop, K. N. Houk, A. Maliakal, *Photochem. Photobiol. Sci.* **2008**, *7*, 1463–1468.

[12] See the Supporting Information for spectra and details.

[13] Fluorescence quantum efficiencies were obtained by a comparison to cresyl violet perchlorate in methanol, see: S. J. Isak, E. M. Eyring, *J. Phys. Chem.* **1992**, *96*, 1738–1742.

[14] The wavelength used as the absorption edge corresponded to the lowest energy absorption with a molar absorptivity $\varepsilon \geq 1000\ \mathrm{L\,mol^{-1}\,cm^{-1}}$.

[15] a) X-ray crystallographic data for **2c**: $C_{45}H_{40}Si$, $M_r = 608.86$; crystal dimensions $0.46 \times 0.40 \times 0.24$ mm; orthorombic space group $Pna2_1$ (no. 33); $a = 34.1011(13)$, $b = 13.6639(5)$, $c = 14.6209(6)$ Å; $V = 6812.7(5)$ Å^3; $Z = 8$; $\rho_{calcd} = 1.187\ \mathrm{g\,cm^{-3}}$; $\mu = 0.100\ \mathrm{mm^{-1}}$; $\lambda = 0.71073$ Å; $T = -100\,^\circ$C; $2\theta_{max} = 55.08^\circ$; total data collected = 58526; $R_1 = 0.0386$ [13955 observed reflections with $[F_o^2 \geq 2\sigma(F_o^2)]$]; $wR_2 = 0.1043$ for 829 variables and 15673 unique reflections with $[F_o^2 \geq -3\sigma(F_o^2)]$; residual electron density = 0.453 and $-0.254\ \mathrm{e\,Å^{-3}}$. b) CCDC-736049 (**2b**) CCDC-736050 (**2c**), CCDC-736051 (**2d**), CCDC-736052 (**2f**) contain the supplementary crystallographic data for this paper. These data can be obtained free of charge from The Cambridge Crystallographic Data Centre via www.ccdc.cam.ac.uk/data_request/cif.

[16] X-ray crystallographic data for **2d**: $C_{49}H_{42}Si$, $M_r = 658.92$; crystal dimensions $0.27 \times 0.20 \times 0.17$ mm; triclinic space group $P\bar{1}$ (no. 2); $a = 9.1190(10)$, $b = 12.8567(14)$, $c = 16.5030(18)$ Å; $\alpha = 70.9187(13)$; $\beta = 83.3738(14)$, $\gamma = 82.2715(15)^\circ$; $V = 1806.6(3)$ Å^3; $Z = 2$; $\rho_{calcd} = 1.211\ \mathrm{g\,cm^{-3}}$; $\mu = 0.100\ \mathrm{mm^{-1}}$; $\lambda = 0.71073$ Å; $T = -100\,^\circ$C; $2\theta_{max} = 52.74^\circ$; total data collected = 14497; $R_1 = 0.0416$ [5703 observed reflections with $[F_o^2 \geq 2\sigma(F_o^2)]$]; $wR_2 = 0.1147$ for 451 variables and 7355 unique reflections with $[F_o^2 \geq -3\sigma(F_o^2)]$]; residual electron density = 0.279 and $-0.244\ \mathrm{e\,Å^{-3}}$. See also ref. [15b].

[17] X-ray crystallographic data for **2f**: $C_{49}H_{42}Si$, $M_r = 658.92$; crystal dimensions $0.27 \times 0.11 \times 0.08$ mm; triclinic space group $P\bar{1}$ (no. 2); $a = 8.5889(11)$, $b = 14.8703(19)$, $c = 15.312(2)$ Å; $\alpha = 71.0863(16)$; $\beta = 81.8475(17)$, $\gamma = 78.8361(17)^\circ$; $V = 1808.4(4)$ Å^3; $Z = 2$; $\rho_{calcd} = 1.210\ \mathrm{g\,cm^{-3}}$; $\mu = 0.100\ \mathrm{mm^{-1}}$; $\lambda = 0.71073$ Å; $T = -100\,^\circ$C; $2\theta_{max} = 53.02^\circ$; total data collected = 14613; $R_1 = 0.0482$ [5103 observed reflections with $[F_o^2 \geq 2\sigma(F_o^2)]$]; $wR_2 = 0.1324$ for 451 variables and 7456 unique reflections with $[F_o^2 \geq -3\sigma(F_o^2)]$]; residual electron density = 0.390 and $-0.367\ \mathrm{e\,Å^{-3}}$. See also ref. [15b].

[18] X-ray crystallographic data for **2b**: $C_{45}H_{40}Si$, $M_r = 608.86$; crystal dimensions $0.66 \times 0.18 \times 0.08$ mm; triclinic space group $P\bar{1}$ (no. 2); $a = 7.6451(14)$, $b = 13.410(3)$, $c = 34.704(7)$ Å; $\alpha = 88.638(2)$, $\beta = 84.211(2)$, $\gamma = 73.839(2)^\circ$; $V = 3399.9(11)$ Å^3; $Z = 4$; $\rho_{calcd} = 1.189\ \mathrm{g\,cm^{-3}}$; $\mu = 0.100\ \mathrm{mm^{-1}}$. $\lambda = 0.71073$ Å; $T = -100\,^\circ$C; $2\theta_{max} = 50.50^\circ$; total data collected = 24203; $R_1 = 0.0732$ [6935 observed reflections with $[F_o^2 \geq 2\sigma(F_o^2)]$]; $wR_2 = 0.2164$ for 863 variables, 72 restraints, and 12272 unique reflections with $[F_o^2 \geq -3\sigma(F_o^2)]$]; residual electron density = 0.514 and $-0.429\ \mathrm{e\,Å^{-3}}$. See also ref. [15b]. The disordered isopropyl groups of molecule B were restrained to have the same geometry as that of one of the ordered isopropyl groups of molecule A by use of the *SHELXL* SAME instruction. Additionally, the Si–C distances of the disordered triisopropylsilyl group were allowed to refine to a common value. Likewise, the C–C distances of the secondary carbon atoms of the minor component were allowed to refine to a common value.

[19] Torsion angles were calculated from the angle between the least squares plane generated from the carbon atoms of each acene.

[20] a) T. Siegrist, C. Kloc, J. H. Schön, B. Batlogg, R. C. Haddon, S. Berg, G. A. Thomas, *Angew. Chem.* **2001**, *113*, 1782–1786; *Angew. Chem. Int. Ed.* **2001**, *40*, 1732–1736. For a discussion of the polymorphs of pentacene, see: b) C. C. Mattheus, G. A. de Wijs, R. A. de Groot, T. T. M. Palstra, *J. Am. Chem. Soc.* **2003**, *125*, 6323–6330; c) C. C. Mattheus, A. B. Dros, J. Baas, G. T. Oostergetel, A. Meetsma, J. L. de Boer, T. T. M. Palstra, *Synth. Met.* **2003**, *138*, 475–481.

[21] Neighboring molecules are not related by symmetry, and the least-squares planes of the acenes in molecule A and B are not parallel, thus requiring an alternative method of measuring the interplanar distances. Distances were measured from every individual acene carbon in molecule A to the neighboring least squares plane generated from the carbon atoms of both acenes in molecule B (and vice versa) to obtain the average value reported.

[22] Interplanar distances were calculated from the distance between the least squares plane generated from the carbon atoms of covalently bonded acenes (the pentacene and its covalently bonded PAH moiety).

[23] J.-L. Brédas, D. Beljonne, V. Coropceanu, J. Cornil, *Chem. Rev.* **2004**, *104*, 4971–5003.

Received: August 5, 2009
Published online: October 21, 2009

